Persistent kallikrein5 activation induces atopic dermatitis-like skin architecture independent of PAR2 activity

Yanan Zhu[1] PhD, Joanne Underwood[2] PhD, Derek Macmillan[3] PhD, Leila Shariff[3] PhD, Ryan O'Shaughnessy[1] PhD, John I. Harper[1] MD FRCP FRCPCH, Chris Pickard[2] PhD, Peter S. Friedmann[2] MD FRCP FMedSci, Eugene Healy[2,4] MB PhD FRCP FRSB , Wei-Li Di[1] MBBS PhD

1. Infection, Immunity, Inflammation and Physiological Medicine Programme, Immunobiology Section, UCL Institute of Child Health, 30 Guildford Street, London WC1N 1EH, UK.
2. Dermatopharmacology, Sir Henry Wellcome Laboratories, Faculty of Medicine, University of Southampton, Southampton General Hospital, SO16 6YD, UK
3. Department of Chemistry, University College London, 20 Gordon Street, WC1H 0AJ, UK.
4. Dermatology, University Hospital Southampton NHS Foundation Trust, Southampton, SO16 6YD, UK

Corresponding Author:
Dr. Wei-Li Di, MBBS, PhD
Senior Lecturer,
UCL Institute of Child Health, Immunobiology Section,
30 Guildford Street, London WC1N 1EH, UK.
Tel: 44 (0)20 79052369
Fax: 44 (0)20 78138494
E-mail w.di@ucl.ac.uk

Conflicts of interest:
none

Declaration of source of funding:
Funding for the study was supported by Sparks and the Livingstone Fund [Great Ormond Street Hospital Children's Charity] and BBSRC.

Abstract

Background: Up-regulation of kallikreins (KLK) including KLK5 has been reported in atopic dermatitis (AD). KLK5 has biological functions which include degrading desmosomal proteins and inducing pro-inflammatory cytokine secretion through protease activated receptor 2 (PAR2). However, due to the complex interactions between various cells in AD inflamed skin, it is difficult to dissect the precise and multiple roles of up-regulated KLK5 in AD skin.

Objective: We investigated the effect of up-regulated KLK5 on the expression of epidermal related proteins and cytokines in keratinocytes and on skin architecture.

Methods: Lesional and non-lesional AD skin biopsies were collected for analysis of morphology and protein expression. The relationship between KLK5 and barrier related molecules was investigated using an *ex-vivo* dermatitis skin model with transient KLK5 expression and a cell model with persistent KLK5 expression. The influence of up-regulated KLK5 on epidermal morphology was investigated using an *in vivo* skin graft model.

Results: Up-regulation of KLK5 and abnormal expression of desmoglein 1 (DSG1) and filaggrin (FLG), but not PAR2 were identified in AD skin. PAR2 was increased in response to transient up-regulation of KLK5, while persistently up-regulated KLK5 did not show this effect. Persistently up-regulated KLK5 degraded DSG1 and stimulated secretion of IL-8, IL-10 and TSLP independent of PAR2 activity. With control of higher KLK5 activity by the inhibitor SFTI-G, restoration of DSG1 expression and a reduction in AD-related cytokine IL-8, TLSP and IL-10 secretion were observed. Furthermore, persistently elevated KLK5 could induce AD-like skin architecture in an *in vivo* skin graft model. .

Conclusion: Persistently up-regulated KLK5 resulted in AD-like skin architecture and secretion of AD-related cytokines from keratinocytes in a PAR-2 independent manner. Inhibition of KLK5-mediated effects may offer potential as a therapeutic approach in AD.

Key messages

- Persistently up-regulated KLK5 induces PAR2-independent IL-8, IL10 and TSLP secretion, causing abnormal keratinocyte growth and AD-like skin architecture.
- Inhibition of KLK5-mediated effects restored DSG1 expression and decreased AD-related cytokine expression, thus suggesting that KLK5 inhibition may be useful as a potential treatment for AD.

Capsule summary

Persistently increased serine protease kallikrein 5 modifies skin barrier proteins, upregulates AD-related cytokine expression and induces AD-like skin architecture. Inhibition of KLK5 may offer potential as a treatment strategy in AD.

Key word

Kallikrein 5, atopic dermatitis, skin barrier, serine protease inhibitor, SFTI

abbreviations

KLK5 (kallikrein), DSG1 (desmoglein 1), PAR2 (protease activated receptor 2), CAP18 (cathelicidin precursor cationic antimicrobial protein 18), AD (atopic dermatitis), NS (Netherton syndrome), FLG (filaggrin), UT (untransduced keratinocytes), AP (PAR2 agonist), TSLP (thymic stromal lymphopoietin), rKLK5 (recombinant KLK5).

Introduction

Tissue kallikreins (KLKs) are a family of fifteen (chymo)trypsin-like serine proteases which function through proteolytic cascades in the skin. Eight KLKs are expressed in the skin with KLK5 being one of the three most important, the others being KLK7 and KLK14[1]. KLK5 is produced as an inactive precursor from keratinocytes and activated by matriptase and KLK14[2,3], but can also undergo self-activation. It is able to activate other KLKs, therefore, KLK5 has been considered to be the initiator of KLK activation cascades within the skin[4].

KLK5 is expressed in the outmost layers of the epidermis, and the importance of its biological function in the epidermal barrier was initially discovered through studies on Netherton Syndrome (NS), a rare severe autosomal recessive skin disorder caused by mutations in the *SPINK5* gene[4,5]. In NS, *SPINK5* mutations cause loss of function of its encoded protein LEKTI, a multi-domain serine protease inhibitor, leading to elevated activity of KLK5. This results in cleavage of intercellular adhesion protein desmoglein 1 (DSG1), causing excessive desquamation of corneocytes and leading to a severely defective skin barrier, a major cause of early neonatal death in NS[6]. In addition to its involvement in DSG1 degradation, KLK5 is able to activate protease activated receptor 2 (PAR2), a subfamily of G protein-coupled receptors, and trigger expression of pro-inflammatory cytokines such as IL-8[7,8]. KLK5 is also involved in the innate immune system within the skin by cleaving the cathelicidin precursor cationic antimicrobial protein 18 (CAP18) at its c-terminus to produce 37 amino acid peptide LL-37, a major antimicrobial peptide with broad-spectrum antimicrobial activity[9].

Up-regulation of kallikreins including KLK5 has been reported in many chronic inflammatory skin diseases including atopic dermatitis (AD)[10,11]. AD is a multifactorial disease caused by complex interactions between genetic and environmental factors, with evidence that irritants (such as those contained in soaps) can further damage the skin barrier and exacerbate the inflammation in AD patients[12]. In the past decade, significant progress has been made in the area of molecular genetics with identification of several genes linked to AD including *SPINK5*, *KLK7* and *FLG*[13-15]. These

findings have led to the proposition that an impaired epidermal barrier is the primary event, allowing percutaneous allergen penetration and causing an enhanced Th2-skewed immune-response[16]. The induced inflammatory response further compromises barrier function, resulting in abnormal expression, activity and assembly of skin barrier related proteins, enzymes and lipids. Aberrant up-regulation of KLK5 in AD skin has been reported[10,11] and increased KLK5 may play a key role in the pathogenesis of the dysfunctional skin. However, due to the complex interactions between various cells in AD inflamed skin, it is difficult to dissect the exact role of up-regulated KLK5 in AD skin.

In this study, we confirmed up-regulation of KLK5 and abnormal expression of KLK5 down-stream molecules DSG1 and filaggrin (FLG), but not PAR2 in AD skin. We also identified significantly increased KLK5 and PAR2 expressions in an *ex-vivo* dermatitis model, but not in the cell model with persistent over-expression of KLK5, illustrating different responses of PAR2 to transient or persistent KLK5 stimulation. We also demonstrated that increased IL-8, IL-10 and TSLP in keratinocytes with persistently expressed KLK5 was independent of PAR2 activity, and that inhibition of KLK5 activity with the serine protease inhibitor SFTI-G reduced cytokine production and normalised DSG1 protein expression. Furthermore, persistent KLK5 over-expression alters keratinocyte behaviour *in vivo*, resulting in epidermal acanthosis similar to that observed in AD skin, indicating a key role for KLK5 in AD pathology.

Materials and Methods

Skin biopsies and haematoxylin and eosin staining (H&E)

Skin biopsies were taken from non-lesional and lesional skin from five AD patients. Five age-matched healthy donors were also obtained. This study was approved by the local ethics committee (LREC number 05/Q0508/106). Skin samples were formalin fixed paraffin embedded, and H&E staining was performed on 6 μm thickness paraffin skin sections using standard histochemistry techniques.

Immunostaining and protein quantification

Immunofluorescence and immunohistochemistry staining were carried out on frozen or paraffin embedded tissue sections using a purified anti-KLK5 mouse polyclonal antibody in 1:500 dilutions (Novus Biologicals, Abingdon, UK), or an anti-DSG1 mouse monoclonal antibody recognizing N-terminal extracellular domain (clone P124) in 1:100 dilutions (2B Scientific Ltd, Upper Heyford, UK), or an anti-FLG monoclonal antibody in 1:100 dilutions (Leica biosystems, Newcastle, UK), or an anti-involucrin mouse monoclonal antibody in 1:1000 (Sigma, Dorset, UK) or an anti-keratin 10 mouse monoclonal antibody (clone number LHP2, a gift from Royal London Hospital, UK). MolecularProbes secondary antibodies conjugated with florescence dye were obtained from Life Technologies (Paisley, UK). The detection of immunohistochemistry used biotinylated secondary antibodies and DAB substrate kit for peroxidase (Vector laboratories, Peterborough, UK). The staining procedures were as described by Di et al[17], and negative controls were performed in each staining with the secondary antibody alone.

The quantification of protein expression and activity in the epidermis was performed based on the staining intensity using software Image-Pro Plus v6.0 (Media Cybernetics, Cambridge, UK). Briefly images of three non-overlapped but adjacent regions in each section were recorded and saved digitally. The epidermis in each image was then highlighted as an area of interest (AOI) and the defined positive staining threshold was applied to the AOIs. The optical counts of positive staining

within AOIs were automatically counted based on the defined threshold and the expression or activity in each AOI was calculated as mean staining intensity /area.

Primary keratinocyte and keratinocyte cell line culture

Primary keratinocytes and fibroblasts were isolated from skin biopsies by incubation with 0.25% trypsin-EDTA (Life Technologies, Paisley, UK) 3 hours for keratinocytes and Serva 50 U/ml collagenase NB6 (Universal Biologicals, Cambridge, UK) 2 hours for fibroblasts. Isolated primary keratinocytes were then co-cultured with lethally irradiated 3T3 mouse fibroblasts and grown in keratinocyte culture media. The media contained equal amount of DMEM and DMEM/Ham F12 (Life Technologies, Paisley, UK) supplemented with 10% FCS (Labtech, East Sussex, UK), 100 IU/ml of penicillin and 100 µg/ml of streptomycin (Life Technologies, Paisley, UK). Human keratinocyte growth supplement was then added to the media at final concentrations of 10 ng/ml of EGF (Bio-Rad AbD Serotec, Oxford, UK), 0.4 µg/ml of hydrocortisone, 5 µg/ml of transferrin, 5 µg/ml of insulin, $2x10^{-11}$ M of liothyronine and $1x10^{-10}$ M of cholera toxin (Sigma, Dorset, UK). Ntert[18], a keratinocyte cell line was cultured in the same keratinocyte media. Fibroblasts were cultured in DMEM supplemented with 10% FCS, 100 IU/ml of penicillin and 100 µg/ml of streptomycin.

Ex-vivo dermatitis model and immunofluorescent staining

Skin from female breast tissue, obtained with informed consent and ethical approval (LREC 07/Q1704/59) following mastectomy was used as an *ex vivo* dermatitis model. The skin, which was surplus to histopathology requirement, was placed in ice cold PBS immediately following removal and stored on ice for a maximum of 2 hours, then placed into a 60 mm petri dish and the epidermal surface carefully blotted dry. Rubber O-rings with a diameter of 8 mm were sealed on to the skin using soft paraffin wax to create wells; care was taken to ensure that paraffin wax was applied only to the area where the O-ring made contact with the skin in order to avoid altering the permeability

of the skin or the protease activity within the epidermis. To prevent the skin from drying out during the incubation period, the remaining space within the petri dish was filled with DMEM, containing 10% FCS, at a depth of approximately 2 mm, ensuring no medium touched the epidermal surface of the skin. Irritant substances and appropriate vehicle controls were applied carefully to separate wells (50 µl solution each) and the skin incubated at 37°C with 5% CO_2 for the required length of time. Following incubation, the entire irritant and vehicle control solutions were aspirated off the epidermis and 6 mm punch biopsies were taken from the treated sites of the skin sample (without removing the rubber O-rings) using sterile biopsy punches. A fresh biopsy punch was used for each treatment to avoid cross-contamination, and the biopsy was removed from within the rubber O-ring using forceps to ensure only treated skin was extracted. The biopsied tissue was placed in a 1.5 ml eppendorf tube and snap frozen in liquid nitrogen. Samples were stored at -80^{o}C until further investigations.

Following removal of skin biopsies from -80°C storage and embedding in Tissue-Tek® optimal cutting temperature medium (OCT) (Sakura Finetek, Thatchem, UK), 8 µm tissue sections were cut on a cryostat, allowed to dry onto poly-L-lysine coated glass slides, then fixed for 10 minutes in ice cold acetone at -20°C. Slides were washed with TBS, blocked for 30 minutes with blocking buffer followed by incubation with primary antibody in TBS overnight at 4°C. Slides were washed for 3 x 5 minutes in TBS, subsequently incubated with secondary antibody for 1 hour in the dark, then washed in TBS for 3 x 5 minutes and, where necessary, counterstained by incubation with DAPI for 10 minutes, followed by a final wash of 3 x 5 minutes in TBS. Coverslips were attached using Mowiol and the samples then visualised by fluorescence microscopy (Axioskop 2 MOT, Zeiss). Slides were magnified at 100x and 400x and images digitally recorded (Axiocam, Zeiss). Slides stained in the absence of primary antibody were used to set the exposure levels to reduce background staining. Images were analysed using ImageJ v1.46 software, with 10 vertical regions of interest (ROI's) from outer to inner surface of the epidermis selected from 1 field of view from 3 consecutive sections for each sample and the contribution from each layer along this measurement

was recorded. The 10 measured ROIs were normalised to 100% and the mean pixel intensity obtained for every 5% of the depth (i.e. from outer to inner surface) of the epidermis. The minimum average pixel intensity for a 5% section in the PBS sample was set at 1 and all other readings for the sample set calculated relative to this value.

Construction of lentiviral vectors and transduction of keratinocytes

Human KLK5 cDNA was cloned into the pCCL lentiviral vector containing upstream spleen focus-forming virus (SFFV) promoter and downstream enhanced green fluorescent protein (eGFP) reporter gene linked to KLK5 via an internal ribosomal entry sequence from the endomyocarditis virus. The vector encoding eGFP alone was used as negative control. Lentiviruses were produced by co-transfecting 293T cells. Infectious lentiviruses were harvested 48 and 72 hours post-transfection, and the culture supernatants were concentrated by ultracentrifugation. The lentivirus concentration were titrated by viral copy number using qPCR and flow cytometry and the titres of eGFP viral vector and KLK5/eGFP viral vector were $8x10^8$ and $4x10^8$ TU/ml, respectively.

Human primary keratinocytes and cell line Ntert were transduced by one round of exposure to eGFP or KLK5/eGFP vectors at an MOI of 10. Transduced cells were subcultured for further experiments.

Intracellular calcium mobilization assay

Measurement of intracellular calcium mobilization was performed using FluoForte Calcium Assay kit (Enzo Life Sciences, Exeter, UK). Mobilization of intracellular calcium was detected utilizing a fluorogenic calcium-binding dye. Keratinocytes were plated in 96-well plates at the density of 1×10^4 cells per well. After 24 hours, the growth medium was removed and 100µl of dye-loading solution was added. The cells were further incubated with the dye-loading solution for 45 min at 37^oC and then 15 minutes at room temperature. The cells were then inoculated with 100 µM of PAR2 activating peptide SLIGKV-NH_2, (Bachem, Cambridge Bioscience, Cambridge, UK), and

intracellular calcium signal was recorded via real-time monitoring of fluorescence intensity at excitation of 530 nm and emission of 570 nm using the microplate reader FLUOstar OPTIMA, (BMG, Lutterworth, UK). Intracellular calcium mobilization was calculated as changes of fluorescence intensity in relative fluorescence units (RFU) and the mobilisation curves were generated by RFU values plotted against the time.

Western blotting

Cells were suspended in a cooled lysis buffer composed of 50 mM Tris-HCl pH 8.0, 150 mM NaCl, 5 mM EDTA, cocktail protease inhibitors and 1 mM PMSF. Samples were incubated for 15 minutes at 4^{o}C and then were centrifuged at 12,000 RPM for 15 minutes. The total protein concentration in the supernatant of lysed sample was determined by Bio-Rad protein assay Kit (Bio-Rad, Hertfordshire, UK). Samples were further diluted 5 times in 0.5 mM Tris-HCl pH 6.8 sample buffer containing 100 mM DTT, 10% SDS, 30% glycerol, 0.001% bromphenol blue. Equal amounts of total protein were loaded in SDS-PAGE. After electrophoresis, proteins were transferred to PVDF membranes and incubated with primary antibody overnight. The following day, membranes were incubated with secondary antibody conjugated with horseradish peroxidase (Sigma, Poole, UK), and signals were detected using the ECL Prime system (GE Healthcare, Bucks, UK). Ponceau red (Sigma-Aldrich, Poole, UK) staining was used as loading control for culture supernatants.

In situ zymography and casein gel zymography

I*n situ* zymography assay using casein-derived substrate measured the total protease activity in the skin. Briefly, the frozen skin sections were rinsed with PBS containing 0.1% Triton X-100 (Sigma-Aldrich, Poole, UK) and incubated at 37°C with 10 μg/ml casein conjugated with BODIPY TR-X (Life Technologies, Paisley, UK) in the buffer containing 10 mM Tris-HCl, pH7.8 in a humid chamber for two hours,. The fluorescent intensity was detected under a fluorescence microscope and quantified using Image-Pro.

Casein gel zymography was used for cells that were cultured in keratinocyte culture media without FCS for 48 hours. The culture media were then collected and concentrated using Amicon centrifugal filter devices (Millipore, Watford, UK). Samples were re-dissolved in non-reducing Novex® Tris-Glycine SDS sample buffer (Life Technologies, Paisley, UK) and separated on 12% polyacrylamide gels copolymerized with casein substrate (Life Technologies, Paisley, UK). After electrophoresis, the gels were soaked in renaturing buffer containing 50 mM Tris, pH 8 and 2.5% Triton X-100 for 1 hour. The gels were then incubated in developing buffer containing 50 mM Tris, pH 8 (Life Technologies, Paisley, UK) at 37°C overnight. Casein degrading activity was visualized when the gels were stained with 1% Coomassie Brilliant blue (Sigma-Aldrich, Poole, UK).

Human cytokine antibody array

The cytokines in culture media collected from the different cell lines were assessed using The Human Cytokine Antibody Array Panel A kit (R&D System, Oxfordshire, UK) according to the manufactory's instruction. A total number of 36 cytokines were measured and the intensities of the blots were quantified by densitometry. As each reference or target protein was blotted in duplicate, mean pixel density from duplicate blots was calculated and normalised by reference blots.

RT-PCR for IL-8

Following RNA extraction using the RNeasy® Plus Mini Kit (Qiagen), a second genomic DNA elimination step was employed to prevent genomic DNA contamination, and cDNA was then synthesised using the RT^2 first strand kit (SABiocience). Quantitative PCR was performed in duplicate wells for each time point using a 7900HT Fast Real-Time PCR System (Applied Biosystems, CA, USA) and the data collected using SDS 2.4 software (Applied Biosystems, CA, USA). The PCR protocol consisted of an initial cDNA denaturation at 95°C for 10 min, followed by 35 cycles of denaturation at 95°C for 15 seconds and annealing and data collection at 60°C for 60 seconds. ΔCT values were calculated using the Ct value for the housekeeping gene 26S and

analysis of fold change in gene regulation was performed using automated Microsoft Excel analysis tools from SABioscience.

Enzyme linked immunosorbent assay (ELISA)

Cells were seeded in 24 well plates and cultured until confluence, then cultured in serum free media for 48 hours before culture media were collected and concentrated using Amicon centrifugal filter devices (Millipore, Watford, UK). The total protein concentration was quantified using Bio-Rad protein assay kit. The level of IL-8 was measured using IL-8 ELISA kit (BD Biosciences, Oxford, UK). TSLP and IL-10 were quantified using ELISA kits from eBioscience (eBioscience, Hatfield, UK). All sample reads were normalized to the total protein concentration.

Bio-engineered skin sheet and grafting onto immunodeficient mice

The methods of generating bio-engineered skin sheet and grafting to mice were as described by Di et al[19]. Briefly, primary human keratinocytes were seeded on the top of a fibrin matrix populated with primary human fibroblasts. After keratinocytes reached confluence, the bioengineered skin constructs were grafted onto the dorsum of 6 weeks old female immunodeficient mice (NMRI strain, Charles River, UK). 8 weeks after grafting, skin samples from grafts were taken post-mortem and formalin fixed and paraffin-embedded or OCT-embedded. H&E staining and immunostaining for KLK5, FLG and DSG1, and zymographics were performed on these tissues.

Results

Increased expression and activity of KLK5 in AD skin

Skin biopsies taken from lesional and non-lesional skin in five children with AD were examined for epidermal morphology and KLK5 expression. Five age-matched normal donor skin biopsies were used as controls. Compared to normal skin, AD lesional skin exhibited epidermal changes including acanthosis, spongiosis, parakeratosis and elongated rete ridges. Non-lesional skin also showed histopathological characteristics consistent with the disease, but far less prominent than those observed in lesional skin (**Figure 1A. a-c**). The expression of KLK5, as detected by immunostaining, was localised in the cornified layer in normal skin, whereas in AD skin, especially in the lesional skin, KLK5 was present in the granular layer and upper stratum spinosum with high staining intensity (**Figure 1A. d-f and Supplementary materials, Figure S1**). Quantification of KLK5 based on mean optical staining intensity/area further demonstrated significant increased expression of KLK5 in both lesional and non-lesional AD skin, compared to the normal skin ($p<0.05$) (**Figure 1B**). As DSG1 is the proteolytic substrate of KLK5, and FLG can be degraded by elastase 2 which is a serine protease activated by KLK5 in the skin[20], DSG1 and FLG expressions were also examined by immunostaining. Both FLG and DSG1 expression were significantly reduced in lesional skin of AD ($p<0.05$) **(Figure 1A. g-i & j-l, Figure 1B**). The protease activity in the skin were further examined by *in situ* staining, and results showed a similar location and staining pattern to KLK5 expression with more diffuse and enhanced fluoresecence intensity in the AD skin (**Figure 1A. m-o, Figure 1B and Supplementary materials, Figure S2**). Although the caseinolytic serine protease assay detects total protease activity, as KLK5 is a major serine protease in the skin[2] and the protease activity closely matched the extent and distribution of KLK5 protein expression, it is likely that KLK5 is a significant contributor to the increased activity of serine protease observed in the AD skin.

Transient up-regulation of KLK5 stimulated PAR2, but persistant activated KLK5 desensitised PAR2

The expression of the KLK5 targeted molecule PAR2 was further examined in the donor skin (n=5) and AD non-lesional and lesional skin by immunostaining. No significant changes in PAR2 expression was noted in lesional, non-lesional AD skin and normal donor skin ($p>0.05$) (**Figure 1A. p-r, Figure 1B**), although there was a fluctuation of PAR2 expression level among individuals. This result suggests that up-regulated KLK5 does not modify PAR2 in AD skin. Considering that the up-regulation of KLK5 was likely to be chronic and persistant in AD skin, we speculated that the response of PAR2 to KLK5 might differ between AD skin and skin with transient KLK5 up-regulation. To determine this, the influence of transiently increased KLK5 on PAR2 was tested using an *ex-vivo* irritant dermatological model in which irritants were applied onto normal skin cultured *in vitro*. Following the application of croton oil or SDS or acetone for 30 minutes on the *ex-vivo* skin model, increased epidermal expression of KLK5 and PAR2 were detected in the epidermis (**Figure 2. a**). Quantification using image analysis confirmed significantly higher expression of both KLK5 and PAR2 across all layers of the epidermis **(Figure 2. b-e)**.

The effect of persistently increased KLK5 on PAR2 was tested in the keratinocyte cell line Ntert (KLK5-Ntert) or primary keratinocytes (KLK5-pKC) ectopically over-expressing KLK5. Cells transduced with eGFP vector alone were used as control (GFP-Ntert or GFP-pKC). The transduction efficiency in both KLK5 transduced cells and GFP transduced cells was nearly 60% as determined by eGFP expression. Overexpression of KLK5 in KLK5-transduced cells and culture media was confirmed by western blotting (**Figure 3. a&c**). The activity of KLK5 was further assessed by zymography. Active KLK5 was detected in the culture media collected from KLK5 transduced cell culture (**Figure 3. d**), but not in cell lysates (**Figure3. b**). KLK5 is synthesized as inactive pre-pro-KLK5 (precursor or zymogene) which is then translocated into the endoplasmic reticulum in cells (see review by Debela M *et al*)[21]. Following the removal of the signal peptide (~30 amino acids), the pre-pro-KLK5 becomes pro-KLK5 that is secreted into the extracellular

space and subsequently becomes activated upon release of its 37 amino acids propeptide from the N-terminus of KLK5. Thus, the KLK5 extracted from the cells would not contain the final activated KLK5 and it is not surprising that there was no positive digested band detected in zymography loaded with cell lysates. In contrast, a digested band was seen in zympgraphy loaded with culture medium from cells over expressing KLK5/eGFP as a result of the culture medium containing the active form of KLK5. Although a ~70kDa band was present on both western blotting and zymography, the intensity of the protein band remained unchanged among cell lysates from untransduced cells, cells transduced with GFP alone and KLK5/GFP, therefore this was considered to represent a nonspecific protein, but having a proteolytic activity on casein-derived substrate.

The durability of KLK5 expression in both KLK5-Ntert and KLK5-pKC was assessed following propagation of transduced cells and there was no decline in KLK5 expression over this time as determined by eGFP expression, indicating persistent KLK5 expression in the KLK5-cell model (**Supplementary materials, Figure S3**). As a previous study showed that PAR2 was mainly expressed in differentiated keratinocytes, the Ntert cell line was checked for differentiation markers keratin 10 and involucrin and results showed positive expression for both proteins (**Supplementary materials, Figure S4**). The activity of PAR2 and a KLK5 down-stream target was then examined in untransfected Ntert (UT-Ntert), GFP-Ntert and KLK5-Ntert by a PAR2-dependent calcium mobilisation assay. Mobilisation of calcium was observed in the untransfected keratinocytes after addition of a PAR2 agonist (AP), and similarly following addition of recombinant KLK5 (rKLK5), albeit slightly later than that induced by AP (**Figure 4. a**), confirming that KLK5 was able to activate PAR2. In contrast, a decline in calcium mobilisation was detected in KLK5-Ntert cells compared to that in GFP-Ntert (**Figure 4. b**). Thus, a different PAR2 dependent calcium mobilisation response was observed in cells with persistent expression of KLK5 versus cells with transient rKLK5 stimulation.

PAR2, like many other receptors, can be desensitized if continuously or repeatly exposed to its agonist[22,23], and these results suggest that persistent over-expression of KLK5 could desensitise the

PAR2 receptor resulting in a lower response of PAR2 to its agonist AP. Since PAR2 desensitisation can be reversed by removal of PAR2 activators, we looked at calcium mobilisation when KLK5-Ntert cells were treated with the serine protease inhibitor SFTI-G, an analogue derived from the naturally occurring substance sunflower trypsin inhibitor 1[24]. Following treatment with 100µM SFTI-G overnight, the PAR2 dependent calcium mobilisation in KLK5-Ntert cells recovered to levels similar to that in GFP-Ntert and untransfected keratinocytes (**Figure 4. c**).

Persistently activated KLK5 induced cytokine expression/secretion despite PAR2 desensitisation

Activated PAR2 induced pro-inflammatory cytokine elevation and secretion, including of IL-8, has been reported[25]. In the *ex-vivo* irritant dermatological skin model, increased IL-8 mRNA expression was detected by RT-PCR within 12 hours following exposure to SDS and to a lesser extent at 12 hours following application of croton oil (**Figure 5. a**). In the KLK5-pKC cells with persistent KLK5 expression, IL-8 protein, measured by cytokine antibody array, was also increased (**Figure 5.b&c**). In addition, IL-10 was elevated in KLK5-pKC cells (**Figure 5. b&c)**, but other cytokines including IL-1, IL-4, IL-6 and IFN-gamma were not (**Supplementary materials, Table S1**). TSLP, a prominent pro-inflammatory cytokine in AD skin also showed increased expression in KLK5-pKC cells as measured by ELISA (**Figure 5. c**). However, increased IL-10 and TSLP were not detected in cells transiently challenged with rKLK5 (data not shown).

Inhibition of persistent KLK5 activity reversed KLK5 effects on DSG1 and cytokine production

To examine the downstream effects of inhibition of persistently raised KLK5 activity, primary keratinocytes transduced with KLK5 (KLK5-pKC) or eGFP (GFP-pKC) were cultured in serum free media inoculated with 100 µM of serine protease inhibitor SFTI-G for twenty-four hours. Although the level of secreted KLK5 in culture media, as determined by western blot, remained

elevated in the KLK5-pKC cells 24 hours post SFTI-G treatment, the expression of full length DSG1 was restored in treated KLK5-cells compared to untreated cells, whereas there was no significant change in the level of DSG1 in GFP-pKC cells before (-) and after SFTI-G (+) treatment, indicating the suppression of KLK5 activity by SFTI-G in the KLK-5 culture (**Figure 6. a**). It was noticed that in KLK5-pKC cells, there was no DSG1 detected. The DSG1 antibody used in the study was a monoclonal antibody (clone P124) recognizing the N-terminal extracellular domain of DSG1 and full length DSG1. Primary keratinocytes were used for untreated as well as treated experiments, and treated cells showed a DSG1 band. Therefore, no DSG1 band in KLK5-pKC cells without SFTI-G treatment was most likely due to DSG1 levels being to too low to be detected and/or the antibody does not recognize the cytoplasm domain of DSG1 alone following the cleavage of the extracellular domain by over-expressed/activated KLK5. Cytokines IL-8, IL-10 and TSLP were also significantly reduced in SFTI-G treated KLK5-pKC cells, compared to untreated KLK5-pKC cells, and these changes were not observed in treated or untreated GFP-cells as confirmed by both cytokine antibody array and ELISA (**Figure 5.b, 6.b&c**, **Supplementary materials, Table S1**).

Keratinocytes with persistent activated KLK5 exhibit an AD-like epidermal architecture

To examine the influence of persistently up-regulated KLK5 activity on epidermal architecture *in vivo*, primary keratinocytes from the non-lesional skin in a patient with AD (AD-pKC), or primary normal keratinocytes ectopically over-expressing KLK5 (KLK5-pKC) or GFP (GFP-pKC) were cultured *in vitro* as bio-engineered skin and grafted onto immuno-deficient mice. 8 weeks post-grafting, the skin from the grafted area was harvested. Grafts generated from KLK5-pKCs and AD-pKC showed AD-like morphology, with acanthosis, mild parakeratosis and enlarged intercellular spaces compared to the GFP-pKC graft (**Figure 7. a-c**). Increased expression of KLK5 and protease activity and decreased DSG1 were observed in both KLK5-pKC and AD-pKC grafts compared to GFP-cell graft (**Figure 7. d-l)**, which were analogous to findings in AD skin. Altered FLG

expression was also detected in KLK5-pKC and AD-pKC grafts, it was more evident in the upper stratum spinosum similar to that seen in the AD skin (**Figure 7. m-o and Figure 1A. h&i).** As the FLG antibody used for the study only detects FLG produced from human cells, the mouse-human skin boundary was easily visible in the FLG stained skin, indicating that the keratinocytes within the grafts were of human origin (**Figure 7. g-i**). In addition, the mouse-human skin boundary images showed an increased thickness of mouse epidermis (acanthosis) next to the grafts generated by KLK5-pKC and AD-pKC, but not by the GFP-pKC, which may have resulted from a paracrine effect of activated KLK5 secreted from these grafts.

Discussion

Up regulated KLK5 together with skin barrier defects in AD has been reported in previous studies[10,11,26], which have shown that both genetic and environmental factors can cause aberrant KLK5 activity. Indeed, as AD shares a number of clinical features with NS, it has been speculated that AD might also share some pathological mechanisms of dysfunctional skin barrier with NS[27,28]. Genome-wide association studies have shown several single nucleotide polymorphisms (SNPs) in *SPINK5* associated with AD, in particular Glu420Lys[28] and functional investigations have further confirmed that Glu420Lys SNP alters SPINK5 encoded protein LEKTI proteolytic activation and results in dysregulation of proteases including the KLKs[29]. Environmental factors that disrupt the skin barrier, including irritants and infection, and trigger KLK5 up-regulation have also been reported[30]. In this study, we have demonstrated that the irritants croton oil and SDS increase KLK5 and PAR2 expression, but that transient KLK5 expression seems to have different effects on PAR2 expression/activity than that observed with persistent KLK5 expression.

KLK5 activation of PAR2 has been demonstrated previously[31] and we also showed rKLK5 activated PAR2 in this study using an intracellular calcium mobilization fluorescence assay. The fluorescence peak induced by rKLK5 was, however, delayed 40-50 seconds compared to the peak induced by the PAR2 agonist (AP). This difference in peak time was likely to be due to the tethered ligand mechanism with regards to maximum rate of PAR2 activation by KLK5. Oikonomopoulou and colleagues[31] have reported that KLK5 activation of PAR2 is a two-step process involving cleavage and tethered ligand binding to the PAR2 receptor, whereas a one-step process is involved in the PAR2 agonist directly binding to the receptor.

The signalling pathway of KLK5-PAR2-NFκB-cytokines has been recognised for more than a decade[32,33], but most studies have been carried out in models with transient exposure to exogenous rKLK5[31]. PAR2 can exhibit desensitization due to continuous or repeated stimulation by its agonist, leading to reduced responsiveness[34]. AD is a chronic skin condition, and up-regulated KLK5 activity in affected skin is most likely to be persistent than transient. However, the examination of

PAR2 activity in skin *in situ* is technically difficult. Currently, the activity of PAR2 is assessed by intra-cellular calcium mobilization in live cells following stimulation/inhibition with its agonist/antagonist. Tissues from AD skin or murine AD models are generally fixed/embedded or snap frozen, and thus are not suitable for use in the calcium mobilization assay. There is an indirect way to check PAR2 activity by examination of PAR receptor internalization, e.g. by tracking GFP-tagged PAR2 fusion protein trafficking[35] or by analysing the distribution of activated (cytoplasmic) and unactivated (cell membrane) PAR2 receptor[36], but these also require cell-culture models rather than skin tissue. However, although the desensitisation of PAR2 in the skin *in situ* cannot be measured directly, previous work by Moniaga and colleagues[37] supports our view that PAR2 is desensitised in AD-like skin lesions. In their study[37], a PAR2 agonist could up-regulate TLSP in murine keratinocytes following transient (one-off) stimulation, but only a marginal increase of TSLP production was noted in the skin of flaky tail mice following repeated topical application of dust mite for 7 weeks; this discrepancy of TLSP production between transient stimulation in cell culture and repeated challenge in mouse skin was probably because the repeated challenge caused PAR2 desensitisation, resulting in low PAR2 activity. Related to this, an *in vivo* study by Briot and colleagues showed that TLSP production was independent of PAR2 activation and that PAR2 was not central to the production of the skin inflammation when there was persistent KLK5 activity[38]. In mice with double knockout of SPINK5-/- and PAR2-/- and high KLK activity, the deletion of PAR2 in the adult double knockout-grafted skin did not result in the reduction of TLSP and did not suppress the skin inflammation[38]. This result suggests that the inflammatory skin in Netherton syndrome and AD is not solely caused by PAR2 activation.

Based on our observations in the AD skin with persistent KLK5 overexpression and the *ex-vivo* irritant dermatological skin model mimicking a transiently increased KLK, we demonstrated that PAR2 had a higher response to transient KLK5 stimulation, but had a weak response to persistent KLK5 stimulation. Interestingly, despite the low activity of PAR2 in cells overexpressing KLK5, these cells up-regulated and secreted pro-inflammatory and Th2-polarizing cytokines, including IL-

8, IL-10 and TSLP, indicating that persistent KLK5 induced IL-8, IL-10 and TSLP. The exact pathway of persistent KLK5 expression/activity induced IL8, IL10 and TLSP secretion in KLK5-pKC remains unclear, and further investigations will be required to elucidate this. The keratinocyte-based nature of our KLK5 over-expressing model, which lacks immune cells, meant that it was not possible to investigate cytokine secretion from immune cells following KLK5 activation, which may explain why our cytokine antibody array data did not show elevation of other cytokines/chemokines reported in AD patients (such as IL-6, IL-4, GM-CSF, IL-1 and TNFα).

The influence of activated KLK5 on epidermal architecture in the *in vivo* human:murine chimeric skin graft model, which showed AD-like skin architecture in grafts generated using cells over-expressing KLK5, further indicated that KLK5 plays a key role in this process. Similar observations have also been detected using a transgenic mouse model over-expressing KLK5[39]. Furthermore, as the human:murine chimeric skin graft model was immunodeficient and maintained in specific pathogen-free environment, our results suggest that the AD-like histopathological features and abnormal barrier protein expression in the epidermis generated by AD-cells and KLK5-pKC cells were a specific consequence of persistent up-regulation of KLK5 in the keratinocytes.

Our study also suggests that increased KLK5 in AD skin should not simply be viewed as a 'biomarker' in this skin disorder, but as a protease which has significant functional impact in this condition. In AD patients, environmental factors can trigger the cytokine cascade and stimulate a Th2-skewed inflammatory infiltrate through the initial defective skin barrier, resulting in susceptibility to allergy or 'atopy' ("outside-inside" aetiological mechanism)[16,40]. The induced inflammatory response further compromises barrier function, causing keratinocyte damage and inducing upregulation of certain molecules, such as KLK5. The initial damage secondary to increased KLK5 forms a vicious cycle of inflammation-induced barrier impairment in AD (outside-inside-outside)[16].

Amongst the currently known inhibitors of kallikreins[41-43], the naturally occurring cyclic peptide SFTI has been extensively investigated due to it being amenable to chemical manipulation which

has allowed for the creation of synthetic variants[44-46]. We used the analogue SFTI-G derived from SFTI[24] to control KLK5 activity and our *in vitro* results showed a normalised DSG1 expression, depletion of depressed PAR2 dependent calcium mobilisation and reduction of IL-8, IL-10 and TSLP. Thus, reducing KLK5 activity could offer a therapeutic option for the treatment of AD, where control of higher KLK5 activity might help to reverse (at least part of) the AD phenotype in patients with this disorder.

Acknowledgements

The authors are grateful to David Rew, University Hospital Southampton NHS Foundation Trust for assistance in procuring skin samples.

Legends

Figure 1. Skin morphology and protein expression in AD

A: Skin sections from normal donor (n=5) and AD skin (n=5) were examined by H&E (a-c), immunostaining (d-l & p-r), and *in situ* zymography (m-o). Green/brown colour represents protein expression or protease activity. Nuclei were stained in blue colour. Scale bar = 50 μm.

B: Quantification of staining intensity (n=3 per sample) was measured by mean staining intensity/area using ImagePro.

Figure 2. **Increased KLK5 and PAR2 expression in *ex-vivo* dermatitis skin model**

Immunofluorescence staining of epidermal KLK5 and PAR2 following application of 3% croton oil and 5% SDS compared with acetone-treated and PBS-treated skin. Quantification of relative KLK5 (b,d) and PAR2 (c,e) expression from stratum corneum to basal layer (0%-100% depth respectively). KLK5 (n=9, n=7), PAR2 (n=7, n=6) for 3% croton oil and 5% SDS respectively.

Figure 3. Characterisation of keratinocyte over expressing KLK5

The expression and activity of KLK5 in cell lysate (a,b) and culture media (c,d) from the cells transfected with KLK5 gene were examined by Western blot (left panel) and gel zymography (right panel). β-actin were used as loading controls. UT = untransduced cells; eGFP = cells transduced with eGFP alone vector; KLK5 = cells transduced with KLK5/eGFP vector and rKLK = activated recombinant KLK5 protein (where rKLK was added directly to the gel as a positive zymography control).

Figure 4. PAR2-dependent calcium mobilisation in keratinocytes

PAR2-dependent calcium mobilisation was measured in untransfected Ntert cells challenged with AP or rKLK5 (a); cells transfected with GFP or KLK5 challenged with AP (b); and cells transfected

584 with GFP or KLK5, treated with SFTI-G and then challenged with AP (c). PBS was used as
585 negative control.
586
587 **Figure 5. Cytokine expression in keratinocytes**
588 Cytokine levels were measured in the *ex-vivo* skin model with transiently up-regulated KLK5 using
589 RT-PCR for IL8 (a); KLK5-pKC cells with persistent KLK5 expression using antibody array blots
590 (b). The IL-8 and IL-10 levels detected by cytokine antibody array and quantified by mean pixel
591 density, and TSLP level measured by ELISA are shown in the bar chart (c). Data in (a) are shown
592 relative to PBS-treated skin.
593
594 **Figure 6. The inhibition of KLK5 by serine protease inhibitor SFTI-G**
595 Primary keratinocytes transduced with GFP or KLK5 gene were treated with 100μM of SFTI-G
596 overnight. KLK5 in culture media and DSG1 in cell lysates were measured by Western blot (a).
597 Cytokine secretions in the culture media following SFTI-G treatment were measured by cytockine
598 antibody array (b) and confirmed by ELISA (c). The symbol * is representative of statistical
599 significance ($p<0.05$) and NS stands for non-significance.
600
601 **Figure 7. Persistent KLK5 activity induced AD-like skin changes**
602 A: Skin graft sections from human:murine skin graft mice were examined for morphology by H&E
603 (a-c), KLK5 (d-f) expression by immunohistochemistry, DSG1 (j-l) and FLG (m-o) expression by
604 immunofluorescence, and protease activity (g-i) by *in situ* zymography. Brown and green colour
605 show protein expression/protease activity and purple and blue colour show stained nuclei. Scale
606 Bar= 50 μm.

References

1. Lundwall A and Brattsand M, Kallikrein-related peptidases, *Cell Mol Life Sci,* 2008 Jul, 65(13):2019-2038.

2. Brattsand M et al., A proteolytic cascade of kallikreins in the stratum corneum, *J Invest Dermatol,* 2005 Jan, 124(1):198-203.

3. Sales KU et al., Matriptase initiates activation of epidermal pro-kallikrein and disease onset in a mouse model of Netherton syndrome, *Nat Genet,* 2010 Aug, 42(8):676-683.

4. Caubet C et al., Degradation of corneodesmosome proteins by two serine proteases of the kallikrein family, SCTE/KLK5/hK5 and SCCE/KLK7/hK7, *J Invest Dermatol,* 2004 May, 122(5):1235-1244.

5. Chavanas S et al., Mutations in SPINK5, encoding a serine protease inhibitor, cause Netherton syndrome, *Nat Genet,* 2000 Jun, 25(2):141-142.

6. Descargues P et al., Corneodesmosomal cadherins are preferential targets of stratum corneum trypsin- and chymotrypsin-like hyperactivity in Netherton syndrome, *J Invest Dermatol,* 2006 Jul, 126(7):1622-1632.

7. Stefansson K et al., Kallikrein-related peptidase 14 may be a major contributor to trypsin-like proteolytic activity in human stratum corneum, *Biol Chem,* 2006 Jun, 387(6):761-768.

8. Steinhoff M et al., Proteinase-activated receptors: transducers of proteinase-mediated signaling in inflammation and immune response, *Endocr Rev,* 2005 Feb, 26(1):1-43.

9. Yamasaki K et al., Kallikrein-mediated proteolysis regulates the antimicrobial effects of cathelicidins in skin, *FASEB J,* 2006 Oct, 20(12):2068-2080.

10. Komatsu N et al., Human tissue kallikrein expression in the stratum corneum and serum of atopic dermatitis patients, *Exp Dermatol,* 2007 Jun, 16(6):513-519.

11. Voegeli R et al., Increased stratum corneum serine protease activity in acute eczematous atopic skin, *Br J Dermatol,* 2009 Jul, 161(1):70-77.

12. Angelova-Fischer I, Irritants and Skin Barrier Function, *Curr Probl Dermatol,* 2016, 49:80-89.

13. Palmer CN et al., Common loss-of-function variants of the epidermal barrier protein filaggrin are a major predisposing factor for atopic dermatitis, *Nat Genet,* 2006 Apr, 38(4):441-446.

14. Vasilopoulos Y et al., Genetic association between an AACC insertion in the 3'UTR of the stratum corneum chymotryptic enzyme gene and atopic dermatitis, *J Invest Dermatol,* 2004 Jul, 123(1):62-66.

15. Walley AJ et al., Linkage and allelic association of chromosome 5 cytokine cluster genetic markers with atopy and asthma associated traits, *Genomics,* 2001 Feb, 72(1):15-20.

16. Elias PM and Schmuth M, Abnormal skin barrier in the etiopathogenesis of atopic dermatitis, *Curr Allergy Asthma Rep,* 2009 Jul, 9(4):265-272.

17. Di WL et al., Human Involucrin Promoter Mediates Repression-Resistant and Compartment-Specific LEKTI Expression, *Hum Gene Ther,* 2012 Jan, 23(1):83-90.

18. Dickson MA et al., Human keratinocytes that express hTERT and also bypass a p16(INK4a)-enforced mechanism that limits life span become immortal yet retain normal growth and differentiation characteristics, *Mol Cell Biol,* 2000 Feb, 20(4):1436-1447.

19. Di WL et al., Ex-vivo gene therapy restores LEKTI activity and corrects the architecture of Netherton syndrome-derived skin grafts, *Mol Ther,* 2011 Feb, 19(2):408-416.

20. Bonnart C et al., Elastase 2 is expressed in human and mouse epidermis and impairs skin barrier function in Netherton syndrome through filaggrin and lipid misprocessing, *J Clin Invest,* 2010 Mar, 120(3):871-882.

21. Debela M et al., Structures and specificity of the human kallikrein-related peptidases KLK 4, 5, 6, and 7, *Biol Chem,* 2008 Jun, 389(6):623-632.

22. Bohm SK et al., Mechanisms of desensitization and resensitization of proteinase-activated receptor-2, *J Biol Chem,* 1996 Sep, 271(36):22003-22016.

23. Stefansson K et al., Activation of proteinase-activated receptor-2 by human kallikrein-related peptidases, *J Invest Dermatol,* 2008 Jan, 128(1):18-25.

24. Shariff L et al., Sunflower trypsin inhibitor (SFTI-1) analogues of synthetic and biological origin via N-S acyl transfer:potential inhibitors of human Kallikrein-5 (KLK5), *Tetrahedron,* 2014, 70:7675-7680.

25. Hou L et al., Immunolocalization of protease-activated receptor-2 in skin: receptor activation stimulates interleukin-8 secretion by keratinocytes in vitro, *Immunology,* 1998 Jul, 94(3):356-362.

26. Komatsu N et al., Multiple tissue kallikrein mRNA and protein expression in normal skin and skin diseases, *Br J Dermatol,* 2005 Aug, 153(2):274-281.

27. Di WL et al., A heterozygous null mutation combined with the G1258A polymorphism of SPINK5 causes impaired LEKTI function and abnormal expression of skin barrier proteins, *Br J Dermatol,* 2009 Aug, 161(2):404-412.

28. Walley AJ et al., Gene polymorphism in Netherton and common atopic disease, *Nat Genet,* 2001 Oct, 29(2):175-178.

29. Fortugno P et al., The 420K LEKTI variant alters LEKTI proteolytic activation and results in protease deregulation: implications for atopic dermatitis, *Hum Mol Genet,* 2012 Oct, 21(19):4187-4200.

30. Torma H, Lindberg M, and Berne B, Skin barrier disruption by sodium lauryl sulfate-exposure alters the expressions of involucrin, transglutaminase 1, profilaggrin, and kallikreins during the repair phase in human skin in vivo, *J Invest Dermatol,* 2008 May, 128(5):1212-1219.

31. Oikonomopoulou K et al., Kallikrein-mediated cell signalling: targeting proteinase-activated receptors (PARs), *Biol Chem,* 2006 Jun, 387(6):817-824.

32. Rallabhandi P et al., Analysis of proteinase-activated receptor 2 and TLR4 signal transduction: a novel paradigm for receptor cooperativity, *J Biol Chem,* 2008 Sep, 283(36):24314-24325.

33. Buddenkotte J et al., Agonists of proteinase-activated receptor-2 stimulate upregulation of intercellular cell adhesion molecule-1 in primary human keratinocytes via activation of NF-kappa B, *J Invest Dermatol,* 2005 Jan, 124(1):38-45.

34. Soh UJ et al., Signal transduction by protease-activated receptors, *Br J Pharmacol,* 2010 May, 160(2):191-203.

35. Ramsay AJ et al., Kallikrein-related peptidase 4 (KLK4) initiates intracellular signaling via protease-activated receptors (PARs). KLK4 and PAR-2 are co-expressed during prostate cancer progression, *J Biol Chem,* 2008 May, 283(18):12293-12304.

36. Gratio V et al., Kallikrein-related peptidase 14 acts on proteinase-activated receptor 2 to induce signaling pathway in colon cancer cells, *Am J Pathol,* 2011 Nov, 179(5):2625-2636.

37. Moniaga CS et al., Protease activity enhances production of thymic stromal lymphopoietin and basophil accumulation in flaky tail mice, *Am J Pathol,* 2013 Mar, 182(3):841-851.

38. Briot A et al., Par2 inactivation inhibits early production of TSLP, but not cutaneous inflammation, in Netherton syndrome adult mouse model, *J Invest Dermatol,* 2010 Dec, 130(12):2736-2742.

39. Furio L et al., Transgenic kallikrein 5 mice reproduce major cutaneous and systemic hallmarks of Netherton syndrome, *J Exp Med,* 2014 Mar, 211(3):499-513.

40. Cork MJ et al., Epidermal barrier dysfunction in atopic dermatitis, *J Invest Dermatol,* 2009 Aug, 129(8):1892-1908.

41. Tan X et al., Toward the first class of suicide inhibitors of kallikreins involved in skin diseases, *J Med Chem,* 2015 Jan, 58(2):598-612.

42. Tan X et al., 1,2,4-Triazole derivatives as transient inactivators of kallikreins involved in skin diseases, *Bioorg Med Chem Lett,* 2013 Aug, 23(16):4547-4551.

43. Teixeira TS et al., Biological evaluation and docking studies of natural isocoumarins as inhibitors for human kallikrein 5 and 7, *Bioorg Med Chem Lett,* 2011 Oct, 21(20):6112-6115.

44. de Veer SJ et al., Mechanism-based selection of a potent kallikrein-related peptidase 7 inhibitor from a versatile library based on the sunflower trypsin inhibitor SFTI-1, *Biopolymers,* 2013 Sep, 100(5):510-518.

45. Swedberg JE et al., Substrate-guided design of a potent and selective kallikrein-related peptidase inhibitor for kallikrein 4, *Chem Biol,* 2009 Jun, 16(6):633-643.

46. de Veer SJ et al., Engineered protease inhibitors based on sunflower trypsin inhibitor-1 (SFTI-1) provide insights into the role of sequence and conformation in Laskowski mechanism inhibition, *Biochem J,* 2015 Jul, 469(2):243-253.

Supplementary materials

Table S1. Quantification of dots by densitometry for cytokine antibody array

Coordinate of the plate	Target/control	Mean pixel density			
		GFP-pKC		KLK5-pKC	
		SFTI (-)	SFTI (+)	SFTI (-)	SFTI (+)
A1,A2	Reference spot	17896	17221	17701	17193
A3,A4	C5/C5a	232	294	245	302
A5,A6	CD40 ligand	216	259	241	226
A7,A8	G-CSF	308	299	327	302
A9,A10	GM-CSF	341	367	319	298
A11,A12	GRO-alpha	18958	19020	19110	19212
A13,A14	I-309	327	381	338	306
A15,A16	sICAM-1	404	394	420	441
A17,A18	IFN-gamma	336	385	312	397
A19,A20	Reference spot	16350	16361	16222	16119
B3,B4	IL-1a	188	226	209	198
B5,B6	IL-1b	217	275	232	202
B7,B8	IL-1ra	15933	15659	15899	16021
B9,B10	IL-2	297	310	268	289
B11,B12	IL-4	322	338	301	297
B13,B14	IL-5	275	311	291	298
B15,B16	IL-6	397	344	380	393
B17,B18	IL-8	15922	15273	22598	16276
C3,C4	IL-10	224	243	8236	268
C5,C6	IL-12 p70	313	289	326	301
C7,C8	IL-13	406	484	415	461
C9,C10	IL-16	359	331	360	314
C11,C12	IL-17	448	429	465	438
C13,C14	IL-17E	385	375	397	408
C15,C16	IL-23	535	521	519	569
C17,C18	IL-27	449	425	456	406

D3,D4	IL-32a	398	331	386	350
D5,D6	IP-10	421	452	409	398
D7,D8	ITAC	415	429	406	466
D9,D10	MCP-1	399	411	394	429
D11,D12	MIF	12868	12525	13310	12806
D13,D14	MIP-1a	275	310	298	322
D15,D16	MIP-1b	393	404	415	438
D17,D18	Serpin E1	18256	18010	18166	18125
E1,E2	Reference spot	17510	17725	17566	17621
E3,E4	RANTES	435	509	466	428
E5,E6	SDF-1	449	399	425	462
E7,E8	TNF-alpha	398	439	412	402
E9,E10	sTERM-1	421	461	435	489
E19,E20	Negative control	275	211	261	293

Legends

Figure S1. KLK5 expression in non-lesional and lesional skin from five AD patients

Skin sections from normal donor (n=5, control 1-5, left panel) and AD patients (n=5, patient 1-5) from non-lesional (middle panel) and lesional (right panel) skin were examined for KLK5 expression using immunohistochemistry. Brown colour represents protein expression and blue colour shows nuclei stain. Scale bar = 100 μm.

Figure S2. *In situ* protease activity in non-lesional and lesional skin from AD patients

Skin sections from normal donor (n=4, control 1-4, left panel) and AD patients (n=4, patient 1-4) from non-lesional (middle panel) and lesional (right panel) skin were examined for total protease activity by *in situ* zymography. Green colour represents protease activity, whereas nuclei are stained blue. Scale bar = 50 μm.

Figure S3. Stability of transgene KLK5 expression in keratinocytes

Primary keratinocytes and Ntert keratinocyte cell line were transduced with KLK5/eGFP transgene and the stability of transgene in cells was assessed by GFP positive cells (GFP+) using flow cytometry. Primary keratinocytes were only monitored for a period of 12 days due to proliferative lifespan of primary cells in *in vitro* culture.

Figure S4. Differentiation markers in Ntert keratinocytes

Keratin 10 and involucrin expression in cell lysates from untransduced Ntert keratinocytes (UT), or transduced with KLK5 (KLK5) or eGFP vector alone (eGFP) were assayed by Western blot. Positive expressions of both proteins indicated a proportion of differentiated cells in the Ntert cell line.

Figure 1A

Click here to download high resolution image

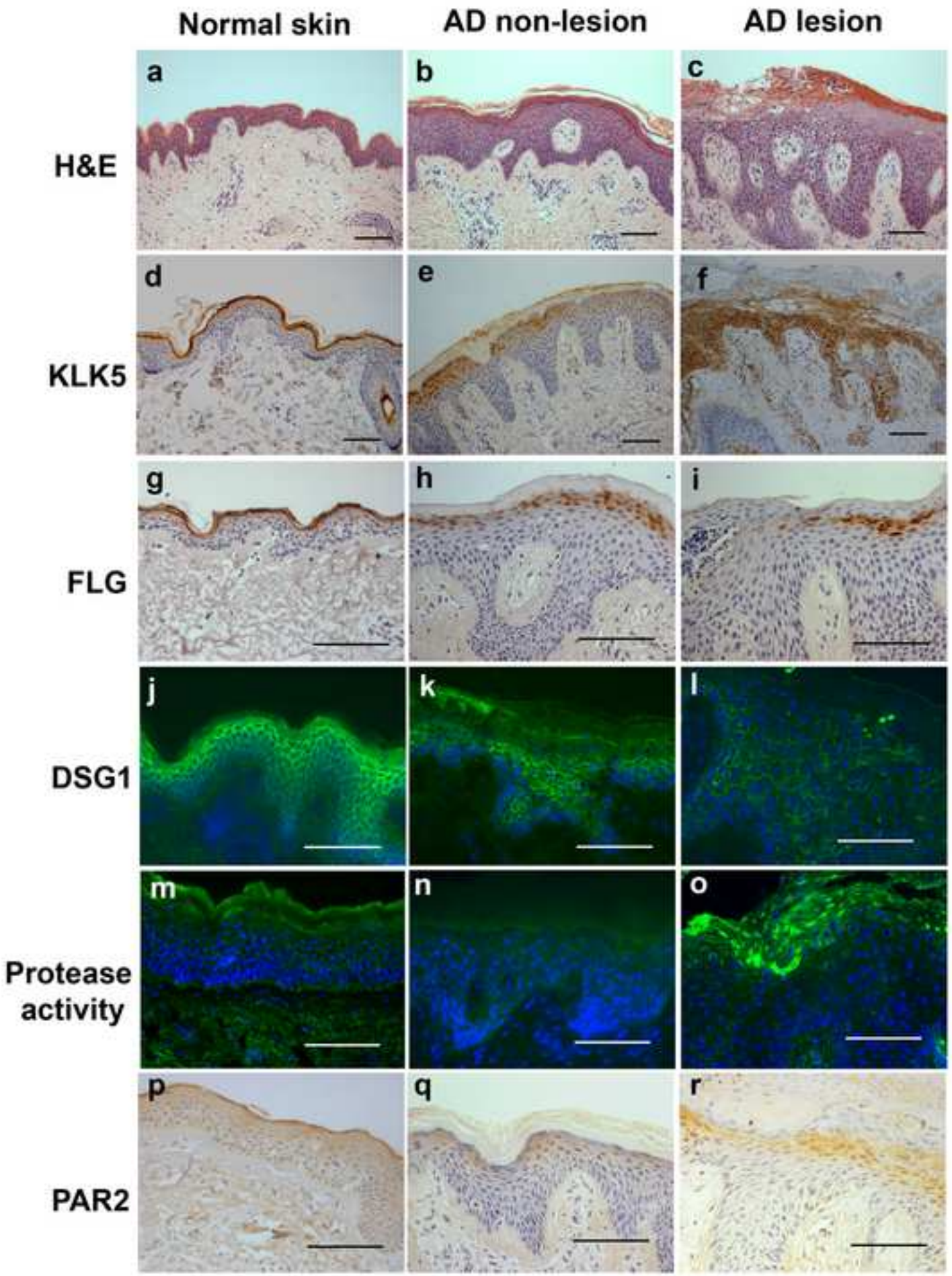

Figure 1B

Click here to download high resolution image

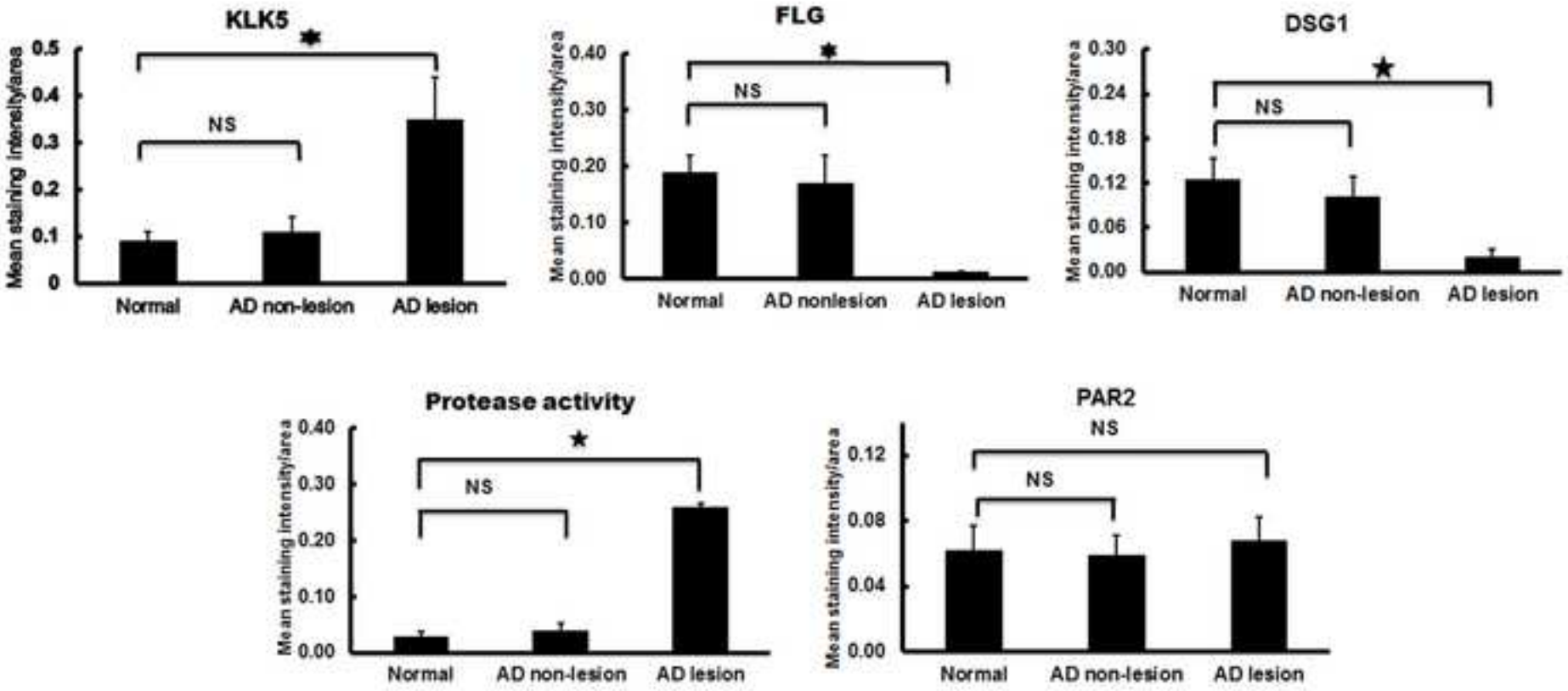

Figure 2

Click here to download high resolution image

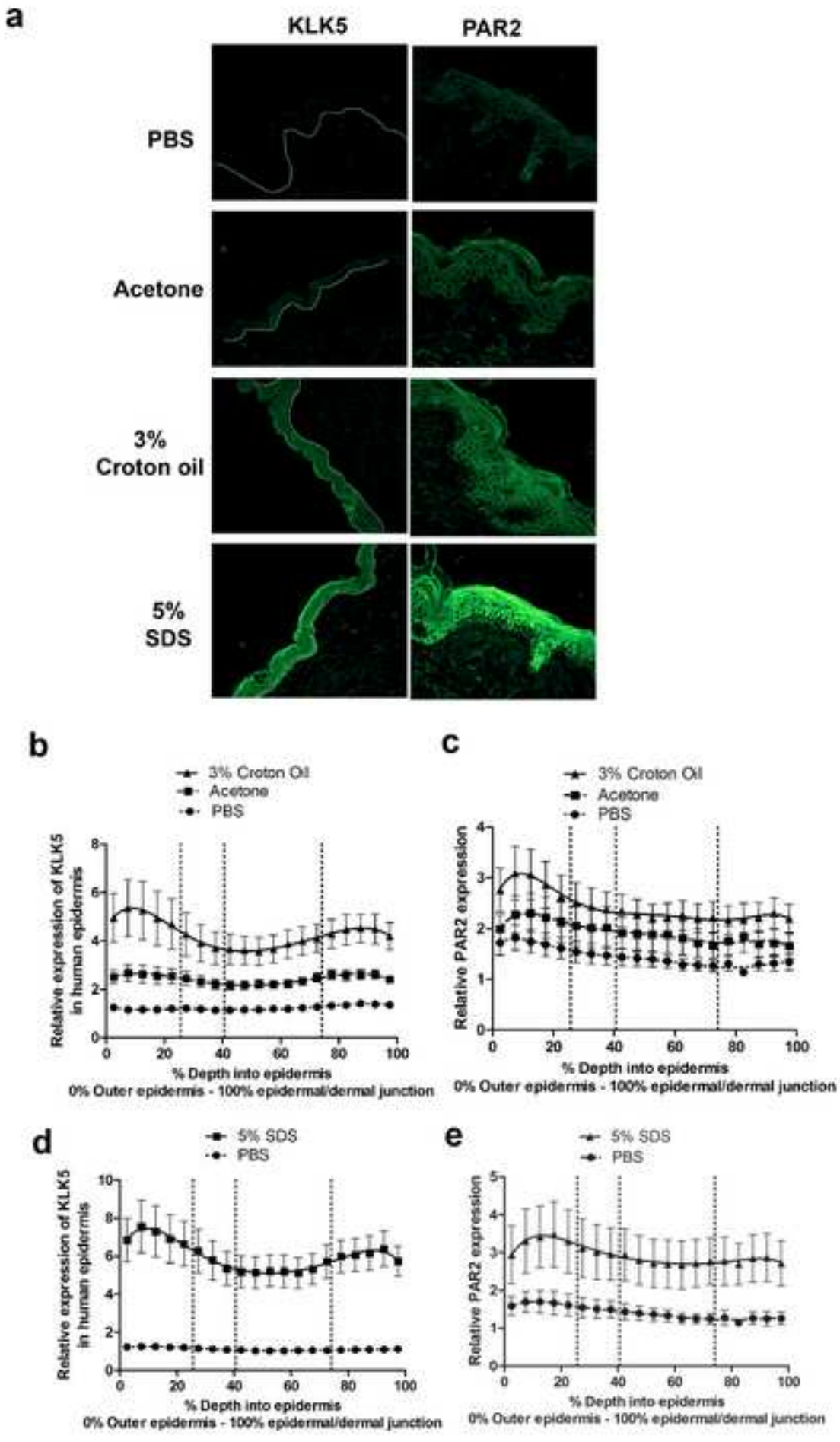

Figure 3

Click here to download high resolution image

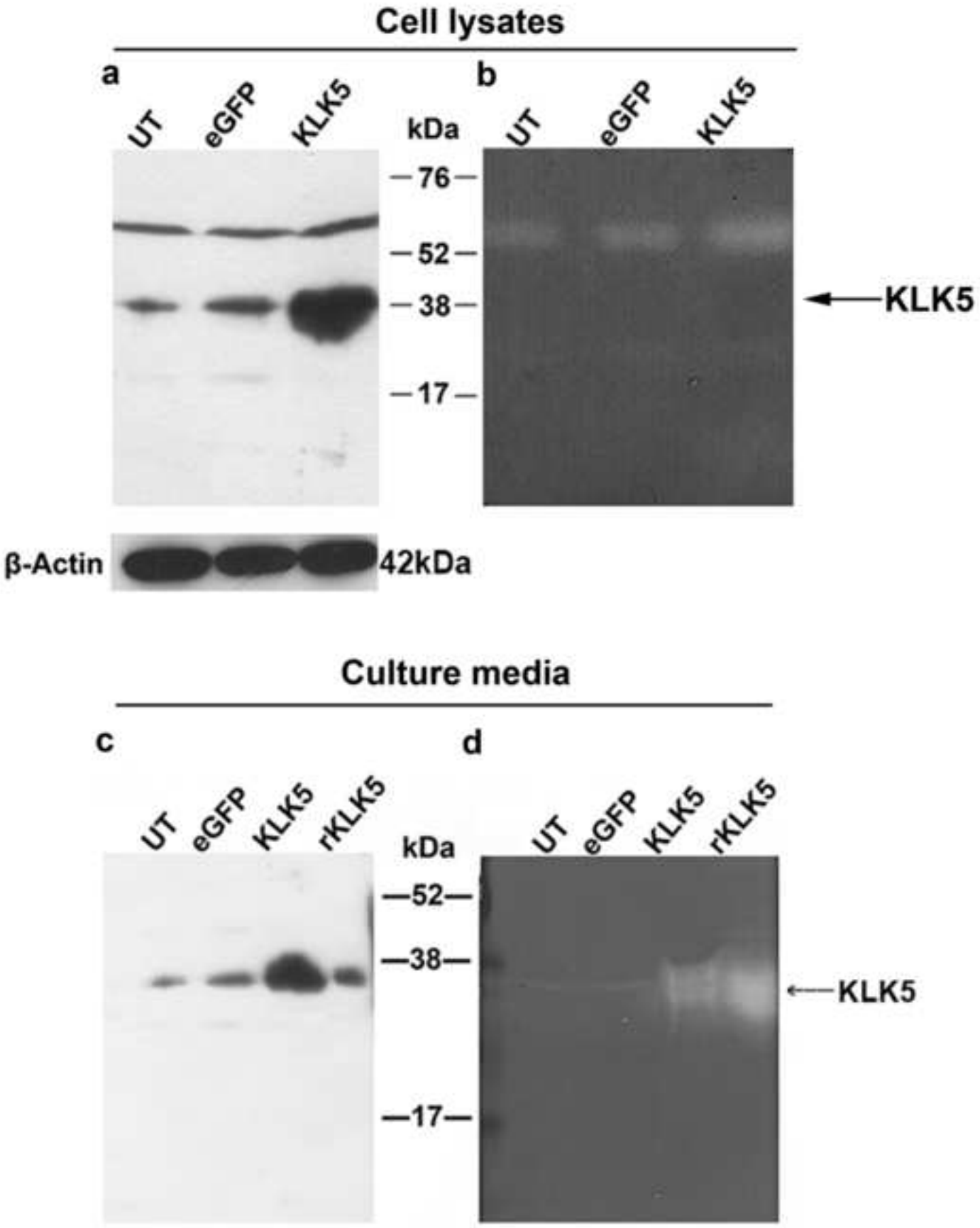

Figure 4

Click here to download high resolution image

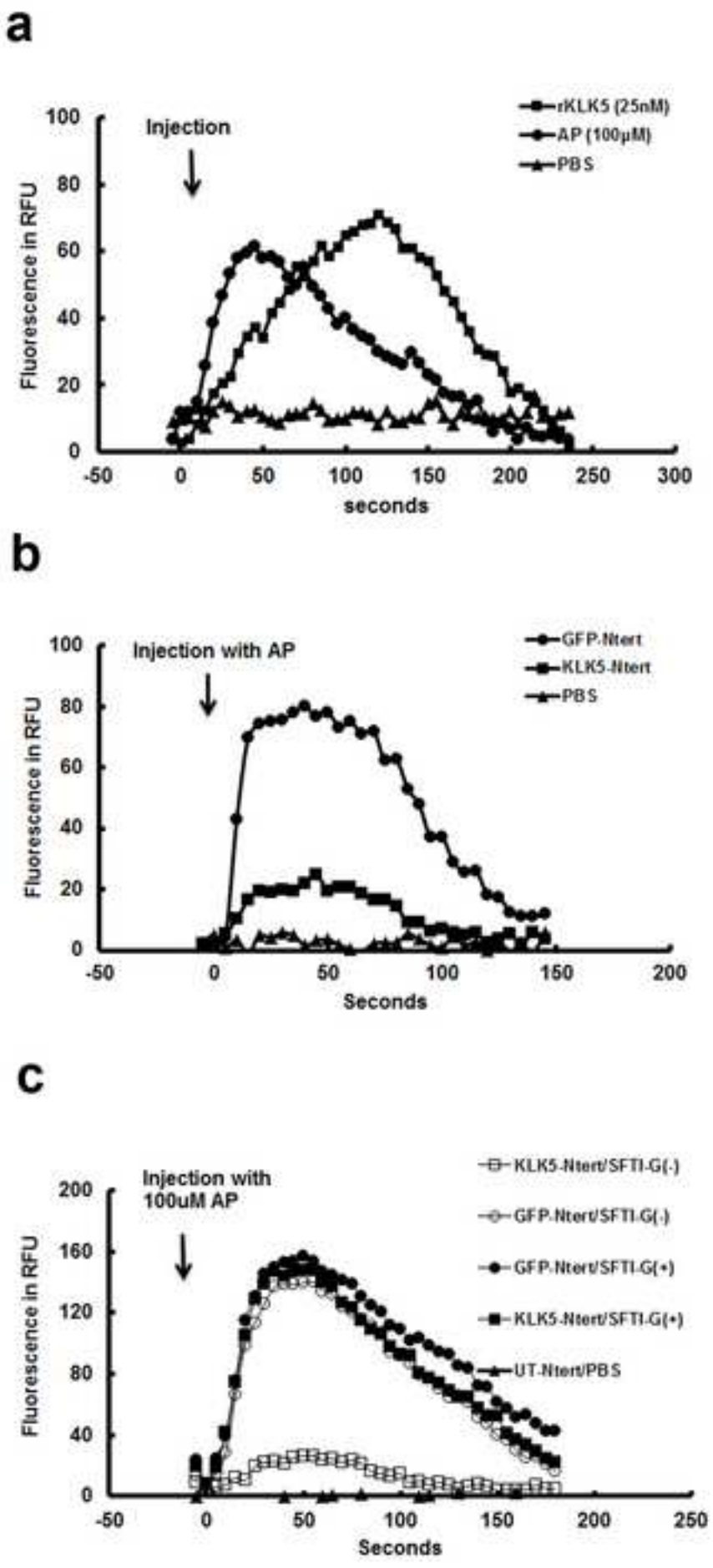

Figure 5

Click here to download high resolution image

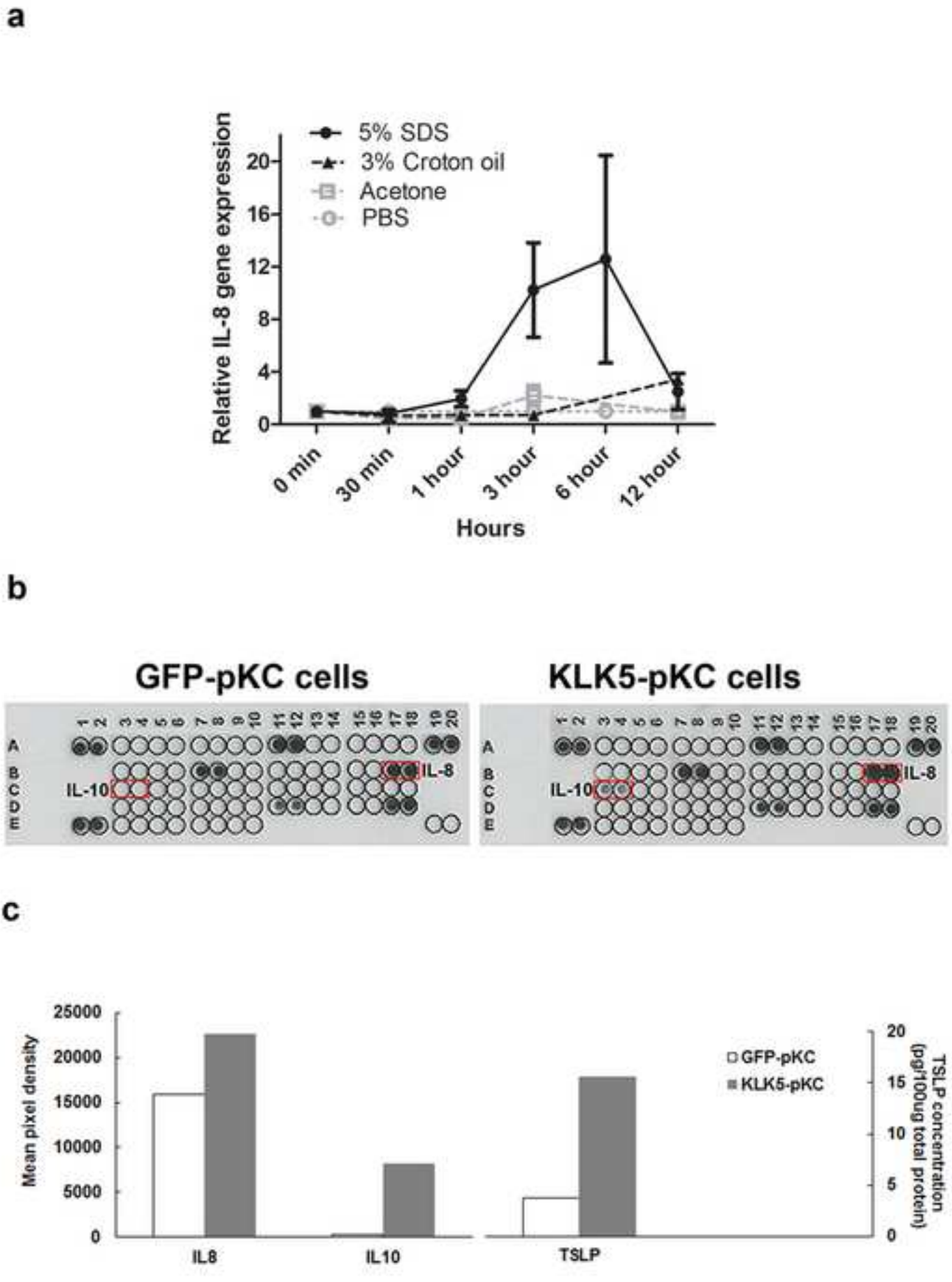

Figure 6

Click here to download high resolution image

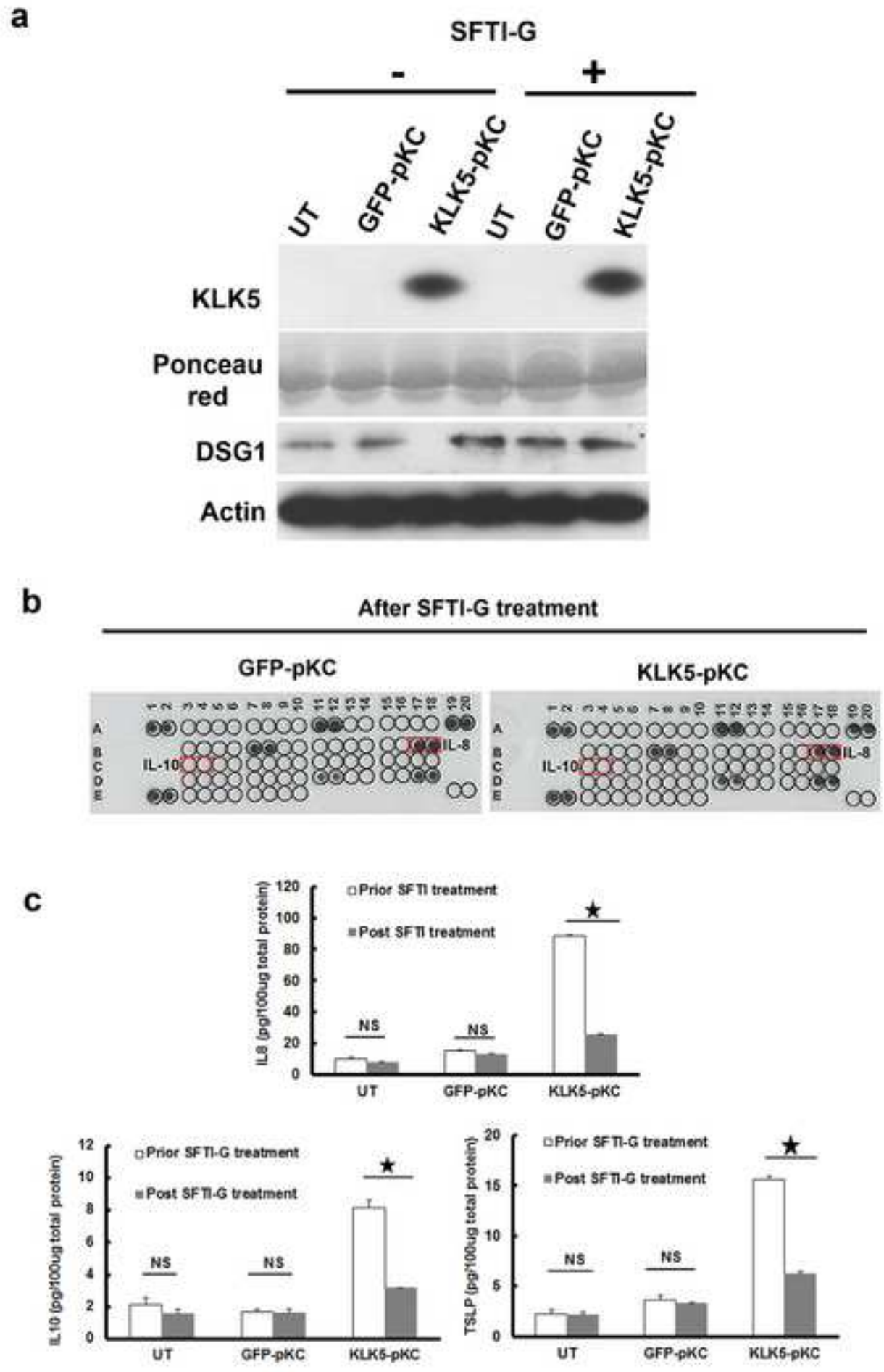

Figure 7

Click here to download high resolution image

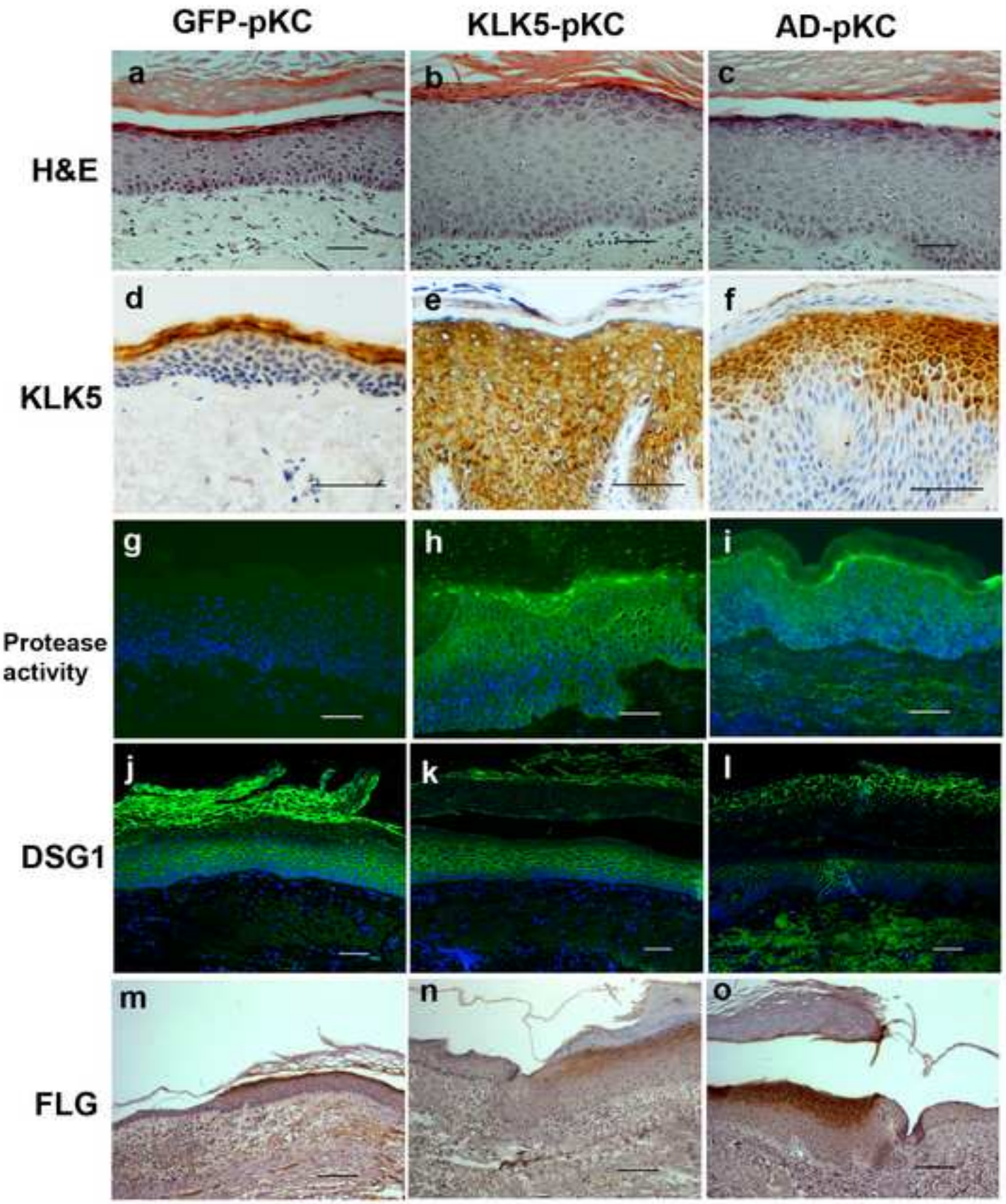

Figure S1

Click here to download high resolution image

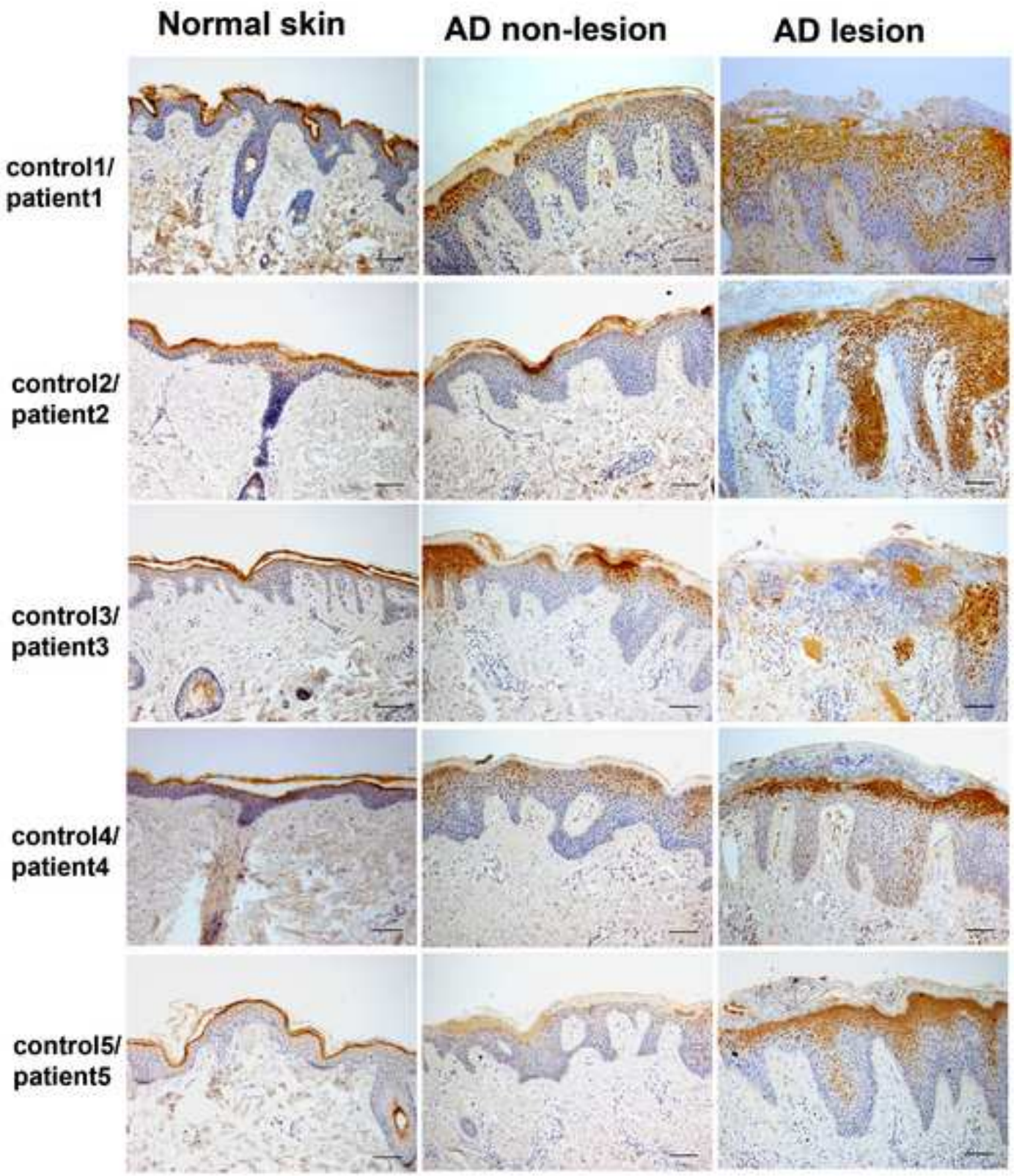

Figure S2

Click here to download high resolution image

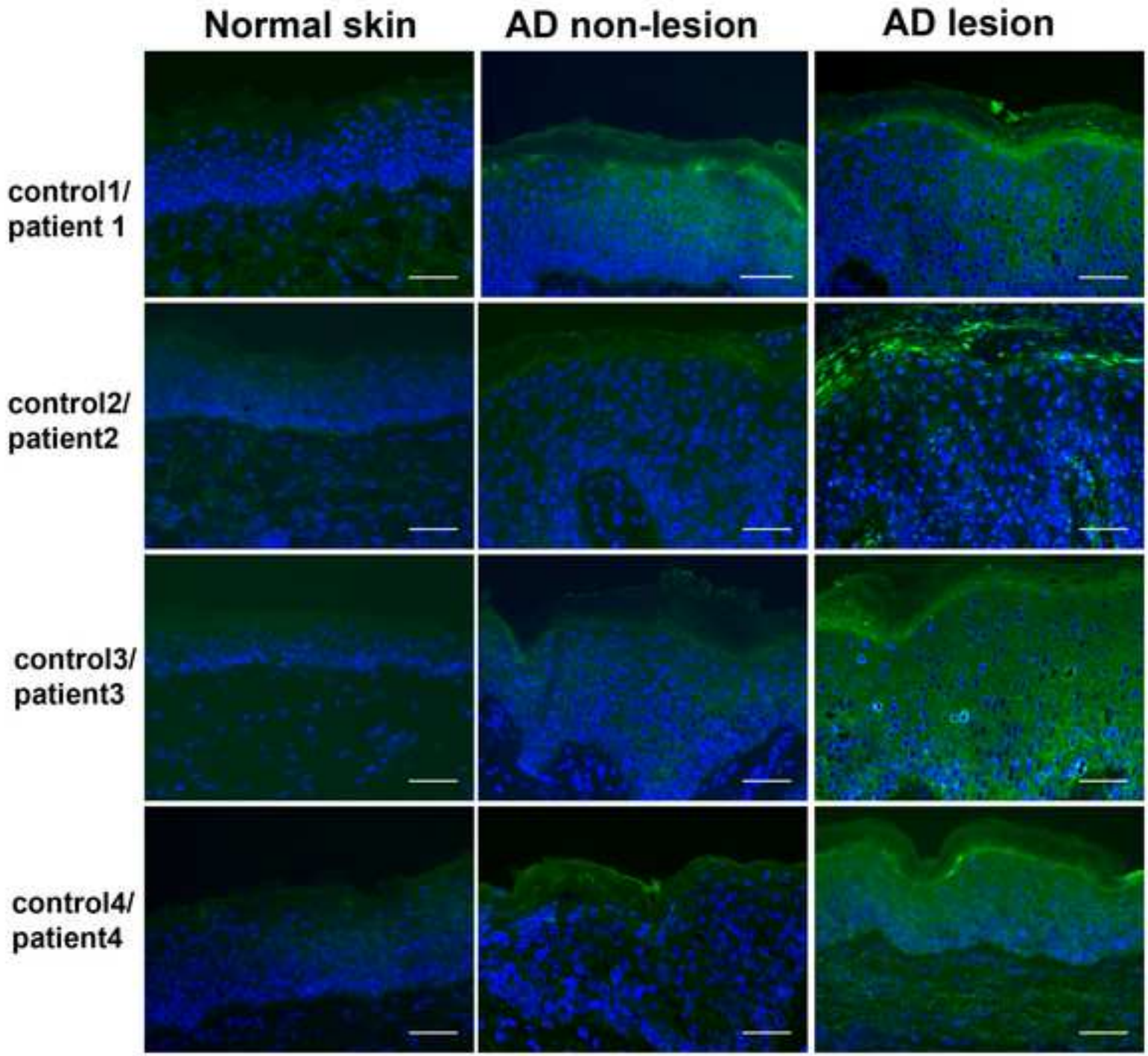

Figure S3

Click here to download high resolution image

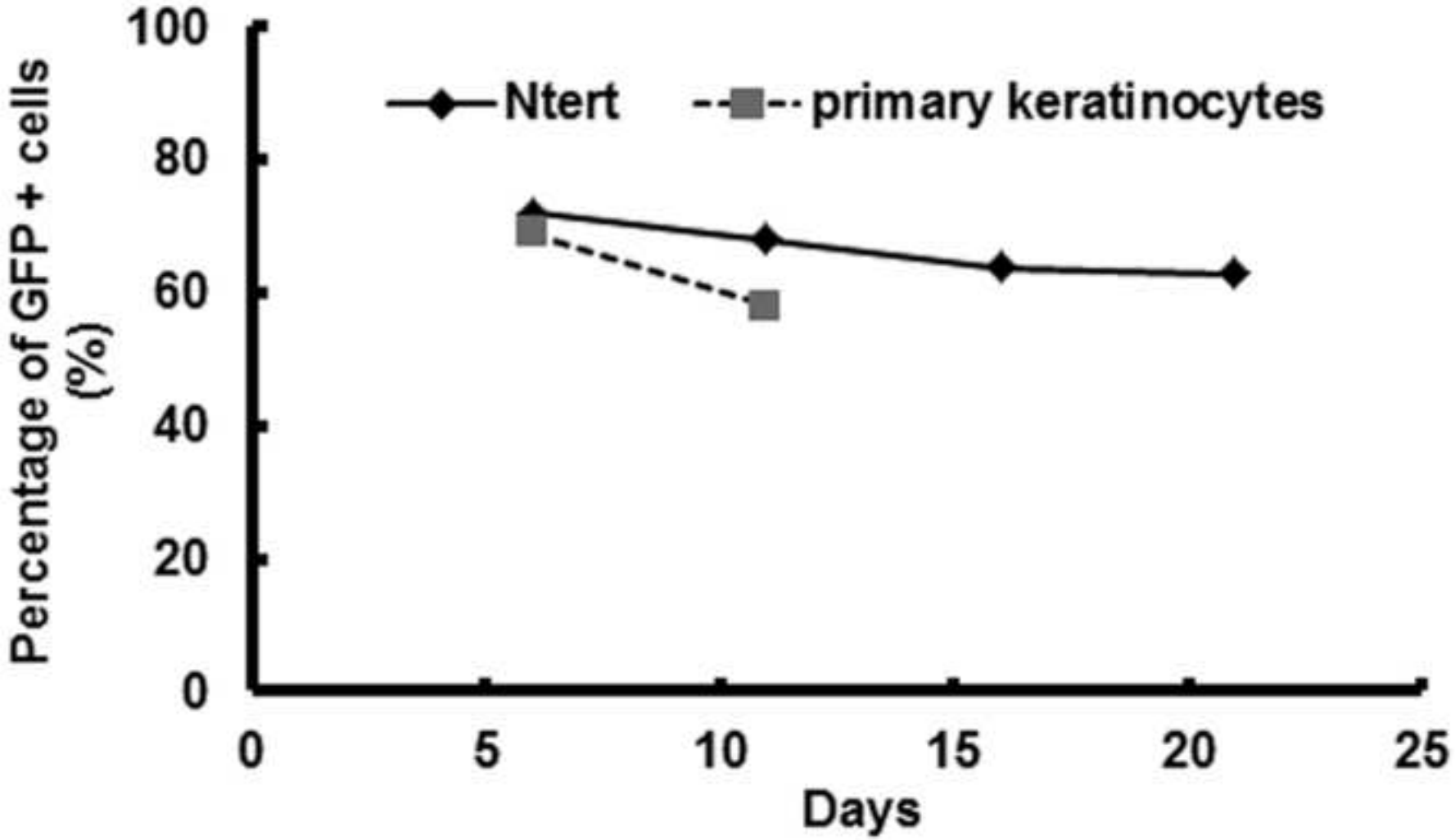

Figure S4

Click here to download high resolution image